Simulations of chemical vapor deposition diamond film growth using a kinetic Monte Carlo model

P. W. May,[1,a)] J. N. Harvey,[1] N. L. Allan,[1] J. C. Richley,[1] and Yu. A. Mankelevich[2]
[1]*School of Chemistry, University of Bristol, Bristol BS8 1TS, United Kingdom*
[2]*Skobel'tsyn Institute of Nuclear Physics, Moscow State University, Leninskie gory, Moscow 119991, Russia*

(Received 19 March 2010; accepted 2 May 2010; published online 8 July 2010)

A one-dimensional kinetic Monte Carlo model has been developed to simulate the chemical vapor deposition (CVD) of a diamond (100) surface. The model considers adsorption, etching/desorption, lattice incorporation, and surface migration along and across the dimer rows. The reaction rates for these processes are re-evaluated in detail and their effect upon the predicted growth rates and morphology are described. We find that for standard CVD diamond conditions, etching of sp^3 carbon species from the growing surface is negligible. Surface migration occurs rapidly, but is mostly limited to CH_2 species oscillating back and forth between two adjacent radical sites. Despite the average number of migration hops being in the thousands, the average surface diffusion length for a surface species—before it either adds to the diamond lattice or is removed back to the gas phase—is <2 sites. β-scission helps to smooth the surface, but is only a relatively minor process removing $<2\%$ of adsorbed species. At low substrate temperature, migration is negligible with film growth being dominated by direct adsorption (Eley–Rideal) processes. The resulting films are rough and spiky, reminiscent of amorphous carbon. With increasing substrate temperature migration increases in significance until for temperatures >1000 K migration becomes the major process by which the surface becomes smoother. Langmuir–Hinshelwood processes are now the dominant growth mechanism, although 30% of growth still occurs via direct adsorption. © *2010 American Institute of Physics*. [doi:10.1063/1.3437647]

I. INTRODUCTION

Chemical vapor deposition (CVD) of diamond is a maturing technology that is beginning to find many commercial applications in electronics, cutting tools, medical coatings, and optics.[1] The CVD process usually involves the gas phase activation of a gas mixture containing a small quantity of a hydrocarbon in excess hydrogen.[2] A typical gas mixture uses a few percentages of CH_4 in H_2 (plus sometimes additional Ar or N_2) and depending upon the growth conditions, substrate properties and growth time, this produces polycrystalline films with grain sizes from ~5 nm to millimeters. Films with grain sizes less than 10–20 nm are often called ultrananocrystalline diamond (UNCD) films; those with grain sizes a few 10s or 100s of nm are nanocrystalline diamond (NCD); those with grain sizes microns or tens of microns are termed microcrystalline diamond (MCD); and those with grain sizes approaching or exceeding 1 mm are single crystal diamond (SCD).

However, to obtain a diamond film with the desired morphology combined with controlled electronic and mechanical properties requires a detailed understanding of the many parameters affecting growth, such as the substrate temperature, gas mixture, process pressure, etc. The difficulty with this is that - even 20 years after diamond CVD was first developed—the exact details of the growth mechanism remain controversial, even though the so-called "standard growth mechanism"[3] developed in the early 1990s is a reasonably robust description of the *general* CVD diamond process. In this model, atomic H, created by thermal or electron-impact dissociation of H_2, is the driving force behind all the chemistry. It is widely accepted[4,5] that the main growth species in standard diamond CVD is the CH_3 radical, which adds to radical sites (dangling bonds) created on the diamond surface following hydrogen abstraction by H atoms. The fraction of surface carbon atoms, F, which support such a radical site is the result of a dynamic equilibrium between H abstraction and H addition reactions which are dependent upon the process conditions, especially the concentration of gas phase atomic H at the surface, $[H]_s$, and the substrate temperature, T_s. F is defined by

$$F = [C_d^*]/([C_d^*] + [C_dH]), \tag{1}$$

where C_d refers to sp^3 carbon in the diamond structure at the surface, and $[C_d^*]$ and $[C_dH]$ are the respective densities of open and hydrogen-terminated surface sites. The three main chemical reactions which govern this equilibrium[6] are

$$H + C_dH \rightleftharpoons H_2 + C_d^*, \tag{R1}$$

$$H + C_d^* \rightleftharpoons C_dH, \tag{R2}$$

$$C_d^* + C_xH_y \rightleftharpoons C_dC_xH_y, \tag{R3}$$

where C_xH_y is a gas phase radical hydrocarbon species, most likely CH_3. Given that (R1) has a forward rate constant k_1 its rate will be given by $k_1[H][C_dH]$. The backward rate (with rate constant k_{-1}) for (R1) is often ignored at low substrate temperatures, but may become important at $T_s > 1000$ °C.

a)Author to whom correspondence should be addressed. Electronic mail: paul.may@bris.ac.uk.

TABLE I. Rate constants in $cm^3\ s^{-1}$ for reactions (R1)–(R3) taken from Refs. 26 and 55.

$k_1 = 3.2 \times 10^{-12}\ T_s^{0.5} \exp(-3430/T_s)$
$k_{-1} = 3.2 \times 10^{-13}\ T_s^{0.5} \exp(-7850/T_s)$
$k_2 = 9.6 \times 10^{-13}\ T_s^{0.5}$
$k_{-2} \sim 0$

Similarly, the forward rate for (R2) is given by $k_2[H][C_d^*]$ and the backward reaction (thermal desorption) can also be neglected. Ignoring the relatively small effects of C_xH_y upon radical site fraction F, (i.e. reactions (R3) and its reverse) we obtain[7]

$$F = 1/\{1 + k_2/k_1 + k_{-1}[H_2]/(k_1[H])\}. \quad (2)$$

In the standard model conditions with only low T_s (so that $k_{-1} \sim 0$[3]) the relationship simplifies to

$$F = 1/\{1 + k_2/k_1\}. \quad (3)$$

Since k_2 is much larger than k_1 (see Tables I and II), this reduces to a limiting value of

$$F = k_1/k_2, \quad (4)$$

at high [H]. Therefore, under typical CVD diamond conditions with $T_s \sim 900$ °C and $1\%CH_4/H_2$ process gases we find that $F \sim 0.1$.

An elevated substrate temperature (typically $T_s > 700$ °C) allows migration of the adsorbed carbon species across the surface until supposedly they meet a step-edge and add to the diamond lattice, or are removed back to the gas phase by an etching process. Another role for the atomic H is to preferentially etch back into the gas phase any adsorbed carbon groups that have deposited as non-diamond phases, while for the most part leaving the sp^3 carbon species behind. It is believed that hydrocarbons C_xH_y with 2 or more carbons ($x \geq 2$) are prevented from contributing to the growth by the "β-scission" reaction[3] which is a rapid, low-energy, efficient process that stops the build-up of long-chained molecules on the growing surface. Therefore, in this standard model, diamond growth is seen as competition between etching and deposition, with carbons being added to and removed from the diamond surface on an atom-by-atom basis.

Surface migration of carbon species is still a somewhat contentious issue, and the mechanism and role it plays in growth remain unclear. Chemisorbed molecular groups, such as CH_2, can, in principle, migrate along or across a dimer row so long as they have an adjacent empty site to move into. These empty sites are created by H abstraction reactions. Therefore, the migration process can be considered to be mediated by the local atomic H concentration since this determines the availability of empty sites. Such *chemical migration* has been considered by a number of groups,[8–10] and the estimated migration length of ~10 Å[9] is consistent with the experimentally observed terrace sizes.[11] Detailed simulations of migration mechanisms on the (100) and (111) surfaces have been performed by Cheesman *et al.*[12] and Larsson *et al.*,[13] respectively, and both suggest low overall barriers for migration resulting in very rapid "hopping" rates at higher T_s values. With all this in mind, a combination of chemical migration, etching and insertion reactions has been used to give a broad explanation for some of the observed morphological patterns of diamond growth, such as apparent step-edge growth, smoothing of diamond surfaces, lateral propagation of lattice steps, and different plane textures.

Our group recently developed a modified version of the standard growth model which considers the effects of all the C_1 hydrocarbon radicals (CH_3, CH_2, CH, and C atoms) on both monoradical and biradical sites on a (100) diamond surface.[14] Our growth model also relies upon surface migration of CH_2 groups along and across the reconstructed dimer rows in order to predict growth rates to within a factor of two of experimental observations but it has an advantage in also being able to predict the average grain size in the resulting polycrystalline film, which can vary from a few nanometers in UNCD films to mm for MCD films.

Despite the successes of both models, evidence for surface migration, nucleation processes, the effects of gas impurities and gas-surface reactions remain sparse and mostly circumstantial. Due to the difficulties of obtaining direct evidence for many of the gas-surface processes by experimental

TABLE II. Concentrations of some of the gas phase species at the diamond surface calculated from a model of the gas phase chemistry (Ref. 14) for a hot filament CVD diamond reactor operating at 20 Torr with 1% CH_4/H_2 gas mixture and filament of temperature 2673 K positioned 6 mm from the substrate. T_s is the substrate temperature and T_{ns} is the calculated gas temperature near the substrate surface. The $[CH_3]$ data are plotted in Fig. 2. Also shown are the values of the fraction of surface radical sites, F, calculated using Eq. (2) which agrees with the values obtained using the KMC program, and with the approximate Eq. (3).

T_s/K	T_{ns}/K	$[H]_s/(10^{14}\ cm^{-3})$	$[H_2]/(10^{17}\ cm^{-3})$	$[CH_3]/(10^{13}\ cm^{-3})$	$[CH_x]/(10^{10}\ cm^{-3})$	F calculation from Eq. (2) and KMC	F calculation from Eq. (3)
573	781	18.0	3.37	2.03	30.0	0.008	0.008
673	857	9.34	2.87	2.50	13.2	0.02	0.02
773	935	5.48	2.50	2.55	8.00	0.038	0.038
973	1094	2.63	1.99	2.00	4.40	0.083	0.089
1173	1266	1.84	1.65	1.44	3.00	0.116	0.152
1373	1442	1.63	1.41	1.13	2.70	0.124	0.215
1573	1621	1.58	1.23	0.92	2.42	0.120	0.274

means, various workers have turned to theoretical models of these interactions. A common approach is that of kinetic Monte Carlo (KMC) simulations. In these, a model of the diamond surface is created and a set of relevant processes and mechanisms are constructed, including those in which C species (CH_3, C_2H_2, etc.) are allowed to strike the surface randomly with a certain impact rate. Some of these will adsorb with a probability given by the rates known from experiment. The KMC simulations then allow migration to occur with the probability of the adsorbed C species jumping to the next site being governed by an activation barrier and the surface temperature. When the C species meets a step-edge, the species may bond to the edge thereby propagating the lattice, with a probability given by the results of detailed calculations previously carried out based upon modeling the geometry, steric effects, and kinetic data. Given sufficient numbers of impinging methyls and sufficient computing time, many layers of diamond growth can be built up.

Early kinetic models of CVD diamond growth[6,15–17] predicted the experimentally observed growth rates but were unable to reproduce some aspects of the morphology, such as the appearance of dimer rows. This is because a major limitation of KMC methods is that they assume advance knowledge of the rates of all the relevant mechanisms. Later KMC models[18–25] became far more detailed and began to reproduce many of the experimentally observed features. One of the best and most recent KMC implementations is that of Netto and Frenklach,[26] which used methyl radicals as the only growth species, with the incorporation into the diamond surface described by means of a ring-opening/closing mechanism. CH_2 migration along and across the dimer reconstructions was included, as well etching of isolated CH_2 groups. The energetics and kinetic data for these reactions were sourced from numerous calculations and experimental measurements.

However, one of the limitations of most reported KMC simulations of diamond growth is the computational expense required. The models of the diamond surface have usually been very detailed, involving the full three-dimensional geometry of the various surface structures at the atomic scale, plus the orientation of the incoming and adsorbed C species. They also involve estimates (some accurate, some little more than educated guesses) for the rates of all the various reactions and their temperature-dependent Arrhenius parameters. Many of the essential kinetic parameters, such as activation barriers for migration and pre-exponential factors are not known with any precision (if at all), and even the identity and concentrations of the species striking the surface are still poorly known. KMC is particularly problematic for diamond growth, since the majority of impacts of gas phase species with the mostly inert H-terminated surface will result in the species bouncing off, with no net growth or etching. Thus, a great deal of computational time is wasted on non-events. Most KMC models in the literature, therefore, often require many days of computing time to simulate the addition of only a few carbons to the lattice and can be quite limited when it comes to understanding "the big picture."

To overcome this problem we developed a simplified one-dimensional (1D) MC model of the growth of diamond films[27] (for a fixed set of process conditions and substrate temperature), with the aim of obtaining insights into the overall growth mechanisms in reasonable timescales. One requirement for our model was that we wished to be able to view the growth of hundreds of layers of the diamond surface in real time using a desktop PC. Although the model was only 1D, the interplay between adsorption, etching/desorption and addition to the lattice was qualitatively modeled using known or estimated values for the rates of each process. Although the topic of surface migration is still somewhat controversial, we included in the model migration of sp^3-bonded CH_2 groups across the (100) surface using a simplified version of the ring-opening mechanism described by Cheesman *et al.*[12]

In the model we also discussed the processes available to surface species that attempt to migrate off the top of step-edges. There are three possibilities: (i) the species simply drops (migrates) down to the bottom of the step-edge (which may be more than one atomic layer deep) and adds to the lattice at that corner; (ii) on attempting to go down the step, enough bonds are broken that the species desorbs back into the gas phase; or (iii) it does not drop down but stays where it is and subsequently migrates back away from the edge (or has a second attempt to jump).[28] These three possibilities (which we somewhat light-heartedly termed "lemmings," "eagles," and "cowards," respectively), are governed by the Ehrlich–Schwoebel potential (ESP), which is the barrier (positive, negative, or zero) which an edge species must overcome to fall down a step-edge.[29,30] Lemmings occur with a zero, negative or small positive ESP, while cowards correspond to an infinite positive ESP. Eagles would occur with a zero or positive ESP but with additional factors to aid etching. Which of these three processes is dominant in diamond growth is arguable, and with no detailed *ab initio* calculations with which to resolve this issue, we previously argued from a geometrical point of view that cowards are the best description for diamond growth. (Later in Sec. IV we shall show that this assumption was incorrect). One outcome of using the cowards scenario was that the calculated diamond surface developed atomic-scale "wedding cake" structures qualitatively similar to those seen using high resolution scanning probe microscopy on real diamond surfaces. For typical CVD diamond conditions, the model predicted growth rates of ~ 1 μm h^{-1}, consistent with experiment, as well as step-edge growth, and it also showed that β-scission is not as important for determining the surface morphology as previously envisaged.

In a follow-up paper[31] we included the possibility of surface defects. Eckert *et al.*[32,33] have modeled in detail the nature, geometry, and types of surface species which are likely to propagate the diamond lattice, or instead, form a number of specific defects. For our simplified approach, we treated all of these defects as being identical, and assigned values for the probability of their appearance following certain surface processes, such as migration and adsorption. Such immobile, unetchable surface defects acted as critical nuclei, allowing the nucleation of new layers, and thus, a greatly increased growth rate when the rate-determining step for growth was new layer nucleation. The defects also insti-

gated the (re)nucleation of a new crystallite, ultimately leading to a polycrystalline film. We showed that using these ideas, we could qualitatively model columnar growth of MCD films as well as NCD and UNCD morphologies.

However, these MC models relied heavily upon the reported literature values for the kinetic parameters of the various surface processes. To extend the MC model further, for example to include temperature dependence, it was necessary to re-examine these values to determine their accuracy and consistency with the microscopic rates for elementary processes at the diamond surface. In this paper we shall re-examine the processes of CH_3 adsorption, surface migration, and etching, and try to rationalize models for their temperature-dependent rates which are then used in a new version of the MC program.

II. THEORETICAL METHODS

A. CH_3 adsorption

Important parameters for the MC program are the concentrations of various gas phase species at the growing diamond surface. These can be obtained from a model for the gas chemistry occurring within hot filament or microwave plasma CVD reactors.[14,34] This model has been tested against laser spectroscopy and *in situ* mass spectrometric measurements. For a given set of process conditions we can use this model to determine, with reasonable accuracy, the concentrations of all the major gas phase species at any position within the reactor. Thus, we can extract the concentration of CH_3 just above the growing surface and extrapolate this to determine the rate of CH_3 species striking the surface per second. The number of CH_3 impacts $cm^{-2}\ s^{-1}$ is given by $[CH_3]_s \times v/4$, where $v = 3757 \times T_{ns}^{0.5}$ $(cm\ s^{-1})$ is the mean thermal velocity of CH_3 and T_{ns} is the gas temperature near the substrate surface. However, most of these impacts will be with a hydrogenated surface C, and so the CH_3 will simply rebound with no reaction. Only those impacts which strike surface radical sites will be important for growth and need be considered in the model. We shall ignore the effects of coadsorbed dopant atoms on the adsorption rate because this is beyond the scope of the present work.[35] Assuming that T_{ns} is approximately the same as the surface temperature, T_s, and that 1 cm^2 of the diamond (100) surface contains $\sim 1.56 \times 10^{15}$ C atoms, then the rate at which CH_3 species are adsorbed per surface radical site is given by

$$CH_3 \text{ adsorption rate}(site^{-1}\ s^{-1}) = \{P \times [CH_3]_s \times (3757 \times \sqrt{T_{ns}})/4\}/1.56 \times 10^{15}, \quad (5)$$

where P is the probability of adsorption onto a radical site (i.e. the sticking probability). The value of P results from a combination of factors that reduce the reaction probability, such as a geometrical factor (g) due to unfavorable collision orientation and a steric-electronic factor (s), such that

$$P = g \times s. \quad (6)$$

The factor s can be estimated since it is known[36] from electronic-spin statistics that, on average, three collisions out of 4 will be on the triplet surface and will not lead to reaction at the high temperatures of diamond CVD. We also know that not all the surface radical sites will be accessible for adsorption (roughly 50%). This leads to an estimated value for s of ~ 0.15. For example, for the standard hot filament deposition conditions[14] given in Table II for $T_s = 1173$ K, and using $g = 0.5$ we get a per site rate of CH_3 adsorption of $\sim 20\ s^{-1}$.

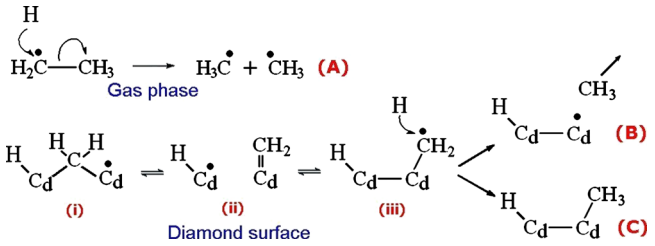

FIG. 1. (Color online) Comparison of the proposed CH_3 etching mechanism on a diamond surface (B) with an analogous gas phase reaction (A). Reaction (C) is H-addition followed by rapid dissipation of energy into the bulk leading a stable pendant CH_3 group without etching. Surface species (i)–(iii) represent different versions of activated CH_2 groups which can interconvert rapidly on the timescale of diamond growth.

B. Etching

During CVD it is believed that gas phase carbon species adsorb onto the growing diamond surface as both sp^2 and sp^3-bonded forms. For NCD or UNCD conditions sp^2-bonded carbon adsorbates may survive for a significant time on the surface, and possibly become "grown-in" to the surface to form defects or act as renucleation sites for new layers or new grains. But for SCD or MCD conditions, where T_s and the surface H atom concentration are high, the etch rate for sp^2 graphitic carbon is ~ 20 times faster than that of sp^3 carbon,[37] and therefore, most, if not all, graphitic carbon adsorbates can be assumed to be etched back into the gas phase before they can have a significant effect upon the surface processes. Therefore, in this paper we shall consider only the removal of the sp^3-bonded adsorbates, and leave modelling of sp^2 defects for later work. The etching of diamond in atomic H atmospheres is known to be very slow ($0.2–0.5\ nm\ h^{-1}$ [38]) but nevertheless has been proposed as a mechanism by which surface smoothing occurs during growth.[39] For our MC model, we require the etching rate for an isolated surface CH_2 or CH_3 group, which may be considerably different to that of the bulk lattice. Simple thermal desorption [i.e. the reverse of reaction (R3)] has been discounted as a removal mechanism due to the relatively low substrate temperatures and the high C–C bond energy. Previously, to obtain a value for the etch rate we followed Netto and Frenklach[26] and assumed that the etching step is simply the reverse of the CH_3 addition process. Here, an adsorbed CH_2 group is removed back into the gas phase (catalyzed by H) as CH_3, leaving behind a surface dangling bond. Netto and Frenklach calculated two etch rates for the two types of bridging site (termed A3 and A4 in Refs. 9 and 49), which we previously averaged[27] to get a mean etch rate.

However, the problem with these etch rates is that the assumptions used in their derivation (by Skokov *et al.*[49]) are questionable. These authors assumed that the H addition reaction to gas phase CH_2CH_3 [Fig. 1, reaction (A)] is a rea-

sonable analogy to those occurring on the diamond surface [Fig. 1, reactions (B) and (C)], and thus, that the known rate for (A) could be used as a good approximation to the etching rate (B). However, in a gas phase reaction such as that shown in reaction (A), the excess vibrational energy deposited in the molecule due to formation of a C–H bond can only escape due to relatively slow radiative or collisional processes, with unimolecular decay due to C–C bond cleavage and hence the formation of CH_3 dominating. But on the diamond surface, the heat released by addition of H to the CH_2 group can rapidly be dissipated into the bulk [reaction (C)], so that only prompt C–C bond cleavage (B) can compete with vibrational deactivation. The rate of etching (B) will be proportional to the relative lifetime of surface species (iii), which is small in comparison with the more probable species (i). The rate will also be related to the proportion of the energy deposited in species (iii) that remains close to the surface, compared to that dissipated within the timescale required to break the C–C bond. Hence, the efficiency of etching by this mechanism can be seen to be inversely dependent on the local thermal conductivity of the diamond surface. Diamond has a very high thermal conductivity, and so energy dissipation is likely to be rapid—however, it is not clear if the thermal conductivity in the near-surface region would be as large as that of bulk diamond. Nevertheless, it is likely that the rate of loss of CH_3 would be reduced to such an extent that etching by this mechanism may be essentially negligible [consistent with both the low etch rates[38] and the low values ($<10^{-6}$) of sputtering yield of C atoms per H atoms seen experimentally].[40] Therefore, we believe that previous MC models (both ours and others[25,26]) may have significantly overestimated the etch rates and, therefore, the importance of etching in controlling surface morphology and growth processes. Until more accurate calculations of these processes can be performed, we have assumed that etching can only occur by the high-energy route of direct breaking of the C–C bond. To model this we used an Arrhenius expression for the rate constant for etching

$$k_{\text{etch}} = A_{\text{etch}} \exp(-E_a/RT_s) \tag{7}$$

where A_{etch} is the collision frequency which we have assumed is the same as that used by Netto and Frenklach (10^{13} s^{-1}) and E_a is the activation energy which we have taken to be equivalent to the C–C bond energy (348 kJ mol^{-1}). With $T_s = 1173$ K, this gives the per site etching rate as 3×10^{-3} s^{-1}, which is a factor of 1000 times slower than most other processes, confirming the notion that such etching processes are (almost) negligible.

C. CH_2 activation and deactivation

From reactions (R1) and (R2) the rate of creation of surface radical sites due to H abstraction is given by

$$\text{Activation rate(sites s}^{-1}) = (k_1[\text{H}]_s + k_{-2})U. \tag{8}$$

The rate constant, k_{-2}, for the reverse of reaction (R2) can be estimated using an Arrhenius expression with pre-exponential factor of $\sim 1 \times 10^{13}$ s^{-1} and activation barrier equivalent to the C-H bond energy (413 kJ mol^{-1}), although it has a value ~ 0 for all values of T_s. The rate of deactivating a surface radical site is

$$\text{Deactivation rate(sites s}^{-1}) = (k_2[\text{H}]_s + k_{-1}[\text{H}_2])A, \tag{9}$$

with U and A being the number of unactivated and activated surface sites, respectively, and the rate constants given in Table I.

D. Surface migration

The migration rate to be considered is that for an activated CH_2 bridging group to move along or across a dimer row. Netto and Frenklach[26] obtained a rate constant for these processes of $\sim 1.5 \times 10^7$ s^{-1} (at $T_s = 900$ °C). More recently, Cheesman *et al.*[12] found the activation barrier for hopping to be slightly less than previously thought, with the values for moving along or across the dimer rows being 145.5 kJ mol^{-1} and 111.3 kJ mol^{-1}, respectively. Taking an average of these, and assuming the same pre-exponential factor as Netto and Frenklach, we obtained

$$k_{\text{hop}} = 6.13 \times 10^{13} \exp(-128\,400/RT_s), \tag{10}$$

for the rate constant of the pure hopping process. However, the activated CH_2 groups will only be able to hop if there is a suitable radical site in a neighboring position. Previously, to obtain the overall rate of migration (per activated surface CH_2 group) we simply multiplied k_{hop} by the chance of a neighboring site being a radical (F), typically 0.1. For standard CVD diamond conditions, this gave values of the rate of migration to be $\sim 1.3 \times 10^7$ s^{-1}, making migration the fastest process by far in the old version of the MC model. It also allowed the CH_2 group to migrate long distances (10–100 sites) across the surface before being etched or adding to the lattice.

However, there are problems with this simple model, since in reality the rate of migration may be significantly slowed by the lack of availability of surface radical sites. Thus, the migration rate is coupled to the H abstraction rate in a more complex way than we (and others) previously accounted for. The new model takes this into account by only allowing migration to occur if *both* the CH_2 is activated and there is a neighboring activated surface site to receive it. There is one further correction which needs to be made to the hopping rate to account for the fact that we are mapping a two-dimensional (2D) process onto a 1D array. Assuming that diagonal hops are disallowed, then, in 2D, an isolated migrating block has four possible positions into which to hop. The probability that one of these sites are unactivated and, therefore, unavailable is $(1-F)$, and the probability that all four are unavailable is $(1-F)^4$. Therefore, the probability that at least one of the sites is available for migration is $\{1-(1-F)^4\}$, and so we need to multiply Eq. (10) by this factor to get the scaled hopping rate for this 1D model. Thus, the rate of migration is given by

$$\text{Migration rate} = \{1-(1-F)^4\} \times k_{\text{hop}} \times M, \tag{11}$$

where M is the number of blocks capable of migrating at that program step.

E. β-scission

Density functional theory calculations[41] for a β-scission reaction on a diamond surface give a value for the enthalpy of C–C bond breaking to release gaseous C_2H_4 leaving behind a surface radical site to be ~180 kJ mol^{-1}. Using simple transition-state theory in the form of the Eyring equation,[42] and assuming that the dissociation energy is approximately equal to the activation Gibbs energy, we get an approximate equation for the rate constant for β-scission of

$$k_\beta = (k_B T_s/h)\exp(-1.8 \times 10^5/RT_s), \quad (12)$$

where k_B and h are the Boltzmann and Planck constants, respectively, which gives values $\sim 2 \times 10^5$ s^{-1} per adsorbed C_2H_5 group for typical substrate temperature $T_s = 1173$ K. This is relatively rapid, and suggests that the C_2H_4 species are removed from the surface rapidly on the timescale of the other processes. The rate for β-scission is then given by

$$\text{Rate of } \beta\text{-scission} = k_\beta B, \quad (13)$$

where B is the number of *activated* 2-block columns in the array at any one time (since β-scission can only occur if the upper block is activated).

F. Migration off the top of step-edges

Previously,[27,31] we adopted the cowards scenario as the default process, which meant that migrating blocks could not jump off the top of step-edges, consistent with a positive Ehrlich–Schwoebel barrier for this process. However, recent quantum mechanical calculations[43] suggest that this barrier is much smaller than previously thought, and of a similar magnitude to the barrier for migration on a flat surface. Therefore, we have now adopted the lemmings scenario as the default process, allowing the blocks to migrate off the top of a step-edge with the same rate as that on the flat, so long as there is a radical site adjacent to the bottom of the step edge upon which the block can land. We realize that this is still a crude approximation to the true process, because our modeled vertical edges are, in reality, sloped (111) surfaces (sometimes called "risers"[44]). Furthermore, the blocks would not simply fall/slide down multistep risers unhindered but would migrate down (and possibly back up again) at a high rate[45] one step at a time. This may become important for step-edges of several blocks in height and may form an interesting issue for future investigation but since for the conditions used here we are mostly dealing with step heights of one or two blocks, we believe the lemmings approximation is sufficient.

III. GROWTH PARAMETERS

In order to test the predictions of the MC model over a range of substrate temperatures we require knowledge of the concentrations of atomic H, H_2, CH_3, and the remainder of the other C_1 hydrocarbon radicals ($C+CH+CH_2$, denoted CH_x) at the growing diamond surface, all as a function of substrate temperature. These parameters have been calculated using the 2D model for a hot filament reactor described in Ref. 14 for a typical set of CVD diamond growth conditions: pressure 20 Torr, 1% CH_4/H_2 gas mixture, filament temperature 2673 K positioned at a distance 6 mm from the substrate. The results of these calculations are given in Table II. The H_2 concentration drops with increasing temperature reflecting the Charles' law behavior for a gas at constant pressure. The concentration of H atoms above the substrate also decreases with T_s but mainly due to the increase in the hydrogen loss probability at the substrate.[46] The CH_x concentrations, which are sensitive to gas phase H-shifting reactions[47] and thus the H/H_2 ratio, also show a monotonic decrease with T_s. In contrast, the CH_3 concentration drops at low substrate temperatures due to three-body recombination with H atoms—a reaction which becomes of increasing importance at low temperatures. As a result the CH_3 concentration rises to a maximum at some intermediate temperature (in our conditions at $T_s \sim 800$ K) then decreases markedly at higher temperatures similar to $[CH_x]$, as plotted in Fig. 2. When using the MC program to investigate the effect of T_s we have performed experiments with two sets of conditions. The first varies T_s but keeps the concentrations of all gas phase species constant at their values for 1173 K. The second uses the correct concentrations of each species from Table II for each T_s value used.

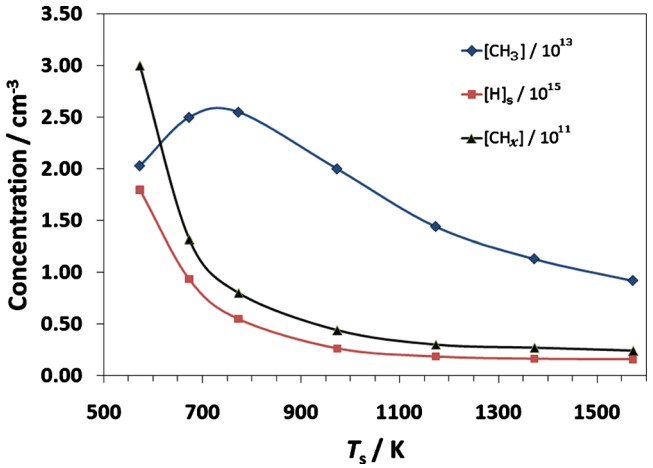

FIG. 2. (Color online) Concentrations of CH_3, $[H]_s$, and $[CH_x]$ directly above the diamond surface calculated using a model of the gas phase species present in a hot-filament reactor[14] as a function of substrate temperature for the conditions outlined in Table II.

IV. THE KMC MODEL

The original model for the MC program is given in Refs. 27 and 31. However, the new version has changed significantly from this—the most important change being that it is now fully stochastic so that the MC program may now be considered a true KMC model. It now operates by comparing the relative rates of each process rather than the probabilities of each process occurring compared to the fastest as in previous versions of the program. As before, in the KMC model the (100) diamond lattice is represented in only 2D, as a cross-section, with the top (growing) surface positioned towards the top of the screen/page (see Fig. 3). Each C atom is represented by a square block within the lattice. New blocks are allowed to land at random (but previously activated) positions on this surface, after which they may adsorb, migrate across the surface, be etched away, or add to the lattice, with

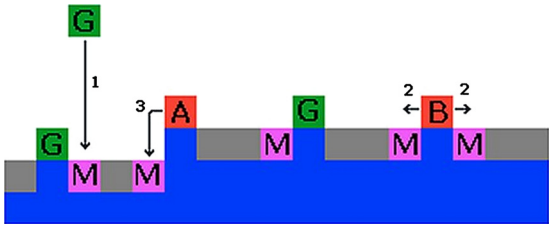

FIG. 3. (Color online) A schematic diagram of the KMC model for the cross-section of the diamond surface and some of the processes occurring there. Magenta blocks (M) represent activated surface radical sites. The (unlabelled) grey blocks represent unactivated, unreactive hydrogenated surface sites, while dark-blue blocks represent bulk subsurface diamond. Green blocks (G) represent immobile CH_3 or CH_2 groups created as a result of adsorption of CH_3 from the gas phase onto M sites (process labeled 1). The red blocks (A) and (B) represent activated CH_2 groups that are able to migrate. In process 2, red block B can jump to the left or to the right since there is an M block at either site. In process 3, red block A cannot jump to the right since there is no M block there. But it can jump to the left and drop down the step-edge (following the lemmings scenario (Ref. 14) since there is an available M block at that corner. Not shown in the figure are the surface activation (grey→magenta or green→red) and deactivation (magenta→grey or red→green) processes.

each process having an independent rate generated at each step of the program based upon the current occupancy of the lattice array. These new blocks represents generic C_1 adsorbing units, which are most probably CH_3 but could be species such as C, CH, CH_2, or even CN, because favorable processes for addition of these species to activated sites are thought to exist. (In fact, C, CH, and $^1CH_2$ can undergo facile processes for addition even to an *unactivated* site[48] but these processes do not play a major role under the present conditions.) Different colored blocks within the array represent different "types" of carbon bonding (see Table III). Carbons that are fully bonded into the bulk diamond lattice are colored dark-blue whereas hydrogenated carbons that form the surface layer are colored grey. A surface radical site is colored magenta and is created as a result of a grey block being "activated" by a successful H abstraction. Green blocks are used to represent pendant CH_3 groups or bonded CH_2 structures that bridge along or across the rows of the dimer pairs on the reconstructed (100) surface [see Fig. 1 (C)]. These are considered to be immobile, although they may rapidly interconvert between the CH_3 and CH_2 forms as a result of H addition/abstraction reactions. An immobile green block can become activated following a successful H-abstraction reaction [the reverse of Fig. 1 reaction (C)]. Such activated blocks [representing Fig. 1, species (i)–(iii)] are colored red, and are allowed to migrate to a neighboring block, so long as there is a surface radical site present there. This change has been implemented because computational models[12,49] suggest that dual activation of the migrating and neighboring sites is required before carbon migration can occur.

The grid has a maximum size of 600×400. At the start of the program, a flat horizontal surface of grey blocks is defined at the bottom of the screen to represent the surface of a single-crystal diamond substrate. The program proceeds by generating a random number, $N(0 \leq N < 1)$, so that at each simulation step a process is chosen with a probability proportional to its rate. The randomly chosen process is carried out, along with any consequences, and a new list of possible processes is generated ready for the next random number comparison. The processes involved are

(a) *Surface site activation*. A grey surface block is activated by H abstraction to form a surface radical site. The grey block then turns magenta and this square is now available for adsorption of an incoming green or a migrating red block. The rate for this process is given by Eq. (8) with U the number of grey blocks in the array at that program step.

(b) *Surface site deactivation*. This is the opposite to (a), in that a magenta surface radical site is deactivated by H addition to become a standard unreactive grey surface site. The rate for this process is given by Eq. (9) with A the number of magenta blocks in the array at that program step.

(c) *Adsorption of a* CH_3 group onto a surface radical site. A new incoming green-colored block (representing a generic C_1 adsorbing unit) is chosen at a random horizontal position above one of the activated surface sites (red or magenta) at the top of the screen, and then allowed to drop vertically until it meets the surface, whereupon it temporarily adsorbs at this position. The rate of impact is calculated from Eq. (5) multiplied by the number of available adsorption sites (i.e., reds + magentas) present on the surface at that program step. The adsorbed green block then has a number of possible pathways (d)–(h), depending upon the local morphology where it landed, and each possible fate is included in the list of possible processes. One other possible fate for it is to stick permanently to form a static, unetchable defect, and this would lead to renucleation events, as discussed in Ref. 31. However, in the work described here we have turned off this option since we are focusing upon the other processes.

(d) *Etching*. Isolated CH_2 bridging units or CH_3 groups

TABLE III. Color codes for the blocks used in the KMC algorithm.

Dark-blue	The subsurface bulk diamond lattice	Immobile, unetchable
Grey	Hydrogenated (unactivated) surface layer	Immobile, unetchable
Magenta	Dehydrogenated activated surface radical site (dangling bond)	Immobile, unetchable
Green	Hydrogenated (unactivated) adsorbed CH_2/CH_3 unit. Equivalent to species (C) in Fig. 1	Immobile, etchable
Red	Dehydrogenated activated adsorbed CH_2 unit. Equivalent to species (i)–(iii) in Fig. 1	Mobile, etchable

may be etched back into the gas phase following H abstraction reactions, with a rate given by Eq. (7) multiplied by the number of etchable blocks (i.e., greens +reds). If successfully etched, the green or red block is then removed and forgotten by the program. With the parameters currently chosen for Eq. (7), the etch rate is almost negligible.

(e) *Activation of adsorbed groups*. As a result of an H abstraction the adsorbed CH_3 becomes an activated CH_2 group (and the green block turns red) which is now capable of migration. The rate for activation is given by Eq. (8) with U being the number of green blocks in the array at that time.

(f) *Deactivation of adsorbed groups*. As a result of H addition onto an activated CH_2 group, the group is "deactivated" and returns to being an immobile (green) CH_2 bridge or pendant CH_3. The rate for this process is given by Eq. (8) with A being the number of red blocks in the array at that time.

(g) *Migration*. An activated (red) CH_2 block may jump sideways left or right one position, so long as there is a (magenta) radical site available to jump into. If migration occurs, the block jumps to the neighboring site (and remains red), and the site it previously occupied now become magenta, since this is now an activated surface site. The rate for this process is given by Eq. (11) where M is the number of red blocks that are allowed to jump.

(h) *Addition to the lattice*. If an adsorbing block lands immediately adjacent to a step edge it will fuse to the lattice and turn grey.[13] This is an example of an Eley–Rideal (ER)-type process. Alternatively, if a migrating red block jumps and lands next to a step-edge, it, too, may fuse to the lattice and turn grey. This is a Langmuir–Hinshelwood (LH)-type process. However, for diamond, the process of attachment of the CH_2 group into an existing sidewall may not be so straightforward since it would require, at least, some sort of surface reconstruction, as well as the breaking and making of several C–H and C–C bonds. Attachment may even require a more complicated process involving a separate reaction, such as the "void filling" reaction proposed by Netto and Frenklach.[26] Other workers[13,50] have modeled the attachment of migrating or adsorbing CH_2 groups to (111) and (100) sidewalls and found that the bond-formation process has a low-energy barrier and is therefore rapid. Therefore, in the model we previously assumed that, upon meeting the bottom of a step-edge a migrating C species attaches permanently with no barrier to this bonding process. We also tested the effect of increasing the barrier to attachment by reducing the attachment probability from 1 down to as low as 0.1, and found that, as expected, this lowered the growth rate but it did not significantly affect the growth morphology.[27] Thus, we shall continue to use 1 as the attachment probability, noting that this is a growth parameter that needs to be more accurately evaluated by detailed atomistic modeling.

(i) *Subsurface layer*. Once a block is no longer part of the surface layer, i.e. it has been buried beneath at least one other layer it turns dark-blue to represent the bulk lattice.

(j) *Critical nucleus formation*. This 1D model assumes that the "critical nucleus" for diamond growth is two adjacent blocks. This is defined as the smallest immobile, unetchable surface feature that provides step-edges suitable for propagating layer growth. Under standard growth conditions a 2-block critical nucleus can be formed by (1) an ER-type process, where an incoming green block adsorbs directly next to a previously adsorbed green or red block causing both of them to bond together or (2) a LH-type process whereby a red block migrates next to a green or red block and they fuse together. These two processes form the basis for new layer nucleation in the absence of defects.

(k) *β-scission*. This is modeled by examining the surface blocks after every program step and identifying any 2-block pillars that may have arisen as a result of blocks landing or migrating. The rate for removal of these via the β-scission mechanism is then calculated using Eq. (13) where B is the number of activated 2-block pillars (i.e. ones which have a red block at the top) present in the array at that time. If the program determines that β-scission has occurred, the 2-block pillar in question is removed from the array, and the exposed underlying block turned magenta. Note that with the standard etching rate [(d) above] being almost negligible, β-scission now represents the only significant mechanism to remove adsorbed sp^3 carbons from the diamond surface.

(l) *Migration off the top of step-edges*. With the lemmings scenario now being adopted as the default process, migrating (red) blocks can readily jump off a step-edge and fall to the bottom (which may be several blocks in height), landing in the bottom corner (so long as the surface block beneath is activated, i.e. magenta). The red block then fuses to the lattice at this corner and becomes grey.

The program was executed until it was stopped manually or until a preset number of layers (typically 300 to provide statistical invariance) had grown, at which point the data were saved. Depending upon the input parameters for the various events, the program took several hours to grow 300 layers (on a Pentium 4 PC). At each step the time taken t_{new} was updated according to

$$t_{new} = t_{old} - \ln(N)/S, \tag{14}$$

where t_{old} is the cumulative time up to the previous step, N is a new random number ($0 \leq N < 1$), and S is the sum of the rates of all possible processes.[51] Thus, the growth rate could be calculated knowing the number of layers of diamond that grew in this time, and that the average C–C distance along a (100) diamond face (i.e. 1 block) is 0.0892 nm.

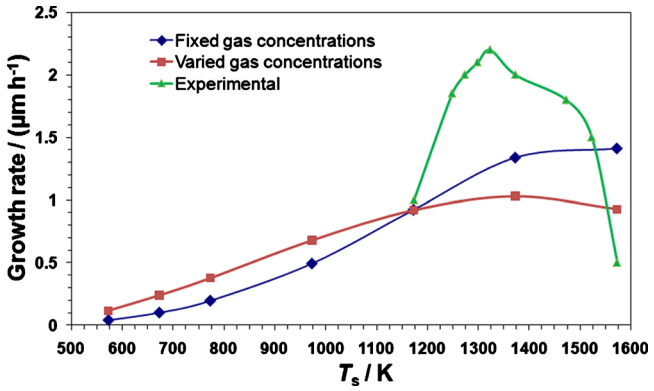

FIG. 4. (Color online) Calculated growth rate for a diamond film using the standard CVD conditions as a function of substrate temperature with gas concentrations fixed for those values at T_s=1173 K and with gas concentrations varying as given in Table II. Also shown are experimental data from a similar (but not identical) system of Kondoh *et al.*[52]

V. RESULTS AND DISCUSSION

Figure 4 shows a plot of the diamond growth rate calculated by the KMC program as a function of T_s for the standard CVD conditions with both constant and varying gas concentrations. At low T_s, the simulation predicts an increasing growth rate with T_s due to an increase in the fraction of surface radical sites, which in turn increases the CH_3 adsorption rate. For fixed gas composition, the growth rate continues to rise with T_s. However, with more realistic varying gas concentrations, the growth rate peaks at $T_s \sim 1350$ K and then drops at higher temperatures. This reflects the drop in $[CH_3]$ at the surface at higher T_s shown earlier in Fig. 2. Also shown are some experimental data by Kondoh *et al.*[52] who used a hot filament system under similar (but not identical) conditions to the ones modeled in our simulations. The magnitudes of the growth rates predicted by our KMC model are within a factor of ~2 of the experimental values, and the trend is also qualitatively reproduced, with the curve peaking at a similar value of T_s. The rapid drop-off in experimental growth rate at $T_s \sim 1300$ K is probably due to restructuring/graphitization of the surface at this high temperature followed by etching of the sp^2 carbons, and since this is not (yet) included in the KMC model the drop-off is not reproduced in our data.

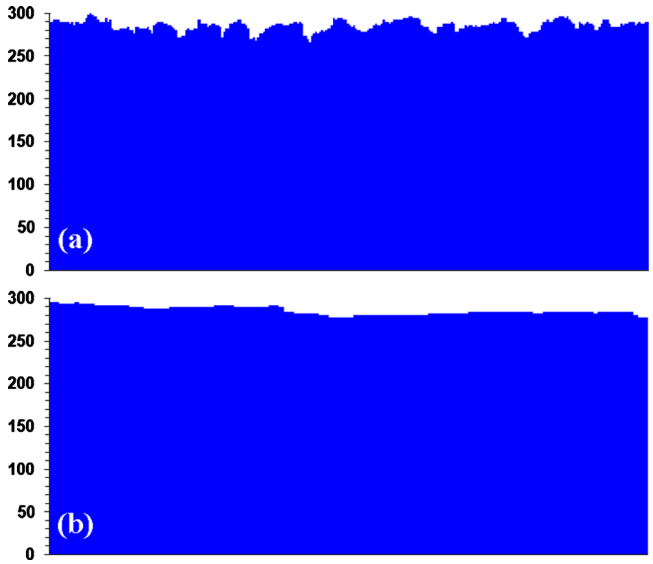

FIG. 6. (Color online) Simulated cross-sections of the diamond surface calculated using the standard conditions given in Table II and substrate temperatures of (a) 773 K and (b) 1373 K. The grid size was 600×300 blocks and the block size was 2×2.

The rms roughness decreases with T_s (see Fig. 5) due to the increased migration of surface species. At low T_s where there is little or no surface migration, growth only occurs via ER processes and the surface is rough, with many spiky protrusions [see Fig. 6(a)]. Such a surface more closely resembles amorphous carbon or graphite sp^2 carbon layers than diamond, which is consistent with experiment. At $T_s > 1000$ K surface migration becomes significant; blocks are now able to migrate down from the top of columns and step-edges producing a smoother surface [see Fig. 6(b)]. LH processes now begin to dominate, although, even at high T_s, ER processes remain responsible for ~30% of the growth (see Fig. 7). The exact ratio between ER:LH processes is a complex function of T_s, the surface roughness and the growth parameters.

The average surface-diffusion length is defined as the mean distance (measured in a straight line) from its initial adsorption site that a migrating species has travelled when its

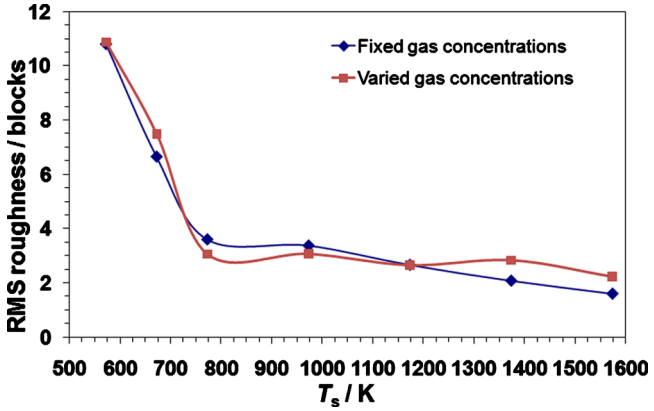

FIG. 5. (Color online) rms roughness of the simulated diamond surface calculated as a function of substrate temperature, for the fixed gas and varied gas concentrations given in Table II.

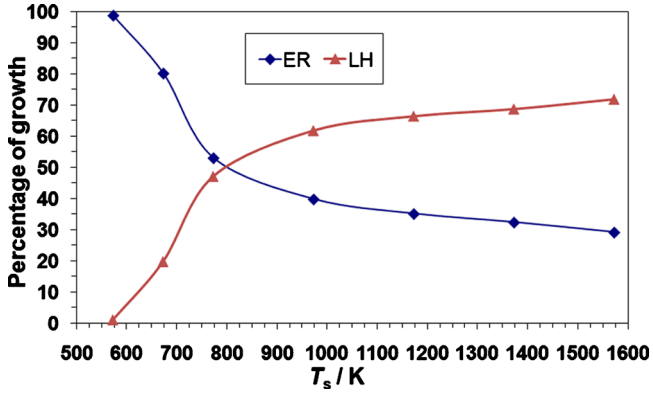

FIG. 7. (Color online) Percentage of growth resulting from ER and LH processes calculated as a function of substrate temperature for the standard diamond growth conditions given in Table II.

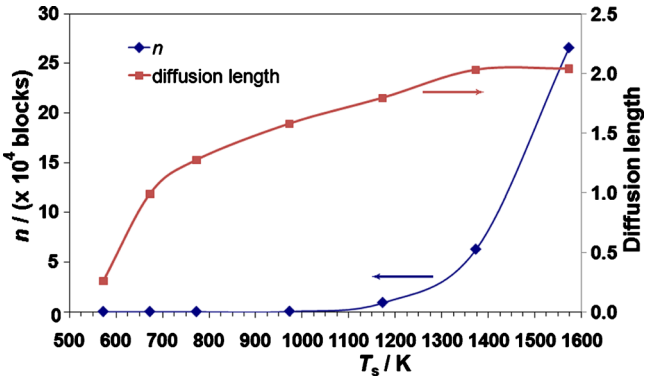

FIG. 8. (Color online) The average number of migration hops, n, per block, and the average surface-diffusion length (distance in lattice sites from the initial adsorption site when the block terminates by adding to the lattice or being etched) calculated as a function of substrate temperature for the conditions in Table II.

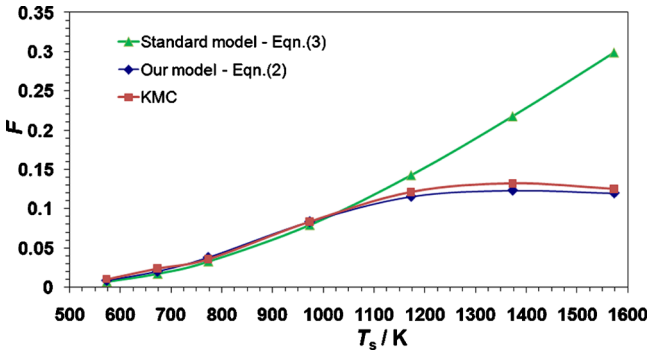

FIG. 10. (Color online) The fraction of surface radical sites, F, plotted as a function of substrate temperature for the standard CVD diamond conditions given in Table II, calculated using the standard model [Eq. (3), which using the values for k_1 and k_2 from Table I approximately follows the expression $F=3.3\exp(-3430/T_s)$], our improved model [Eq. (2)], and from the output of the KMC program.

migration is permanently terminated by processes such as etching, attachment to the lattice, etc. This diffusion length is a function of T_s (see Fig. 8), mainly through the increase in migration rate. However, the diffusion length remains very small, <2 blocks (equivalent to surface lattice sites) for all temperatures tested. This is despite the average number of hops made by the migrating species being as high as 10^5 (see Fig. 8). The reason for this is that the migrating CH_2 species hop back and forth rapidly between two adjacent radical sites, and only rarely migrate beyond this when a third surface site activates adjacent to one of the previous two. This new insight into migration shows that the surface-diffusion length is, indeed, severely limited by the lack of availability of surface radical sites, and it is this reduced diffusion length which gives rise to the general features of the surface morphology.

β-scission reactions play only a small part in smoothing the film surface, as can be seen from Fig. 9. The number of β-scission reactions has a maximum value of only $\sim$1.6% showing that this process is only a minor contributor to surface smoothing. This value is somewhat larger than those calculated for SCD/MCD conditions in our previous paper[27] ($\sim$0.12%) but nevertheless confirms that β-scission is perhaps less important than previously thought. The curve peaks at $T_s\sim1000$ K due to a balance between two competing

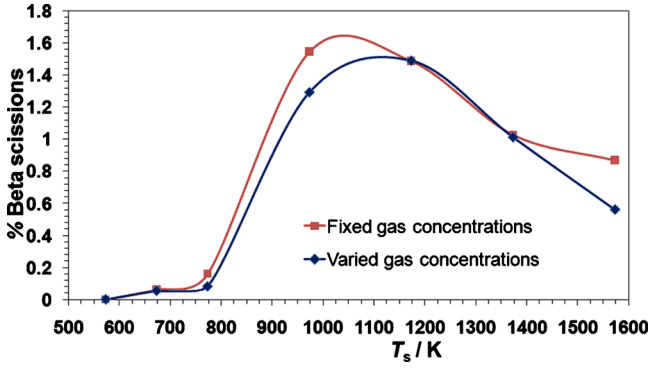

FIG. 9. (Color online) The percentage of β-scission reactions (i.e. the number of blocks that undergo β-scission divided by the total number of blocks that adsorbed) as a function of substrate temperature, for fixed and varied gas concentrations as in Table II.

rates which both increase with T_s: the β-scission reaction rate and the migration rate. At low temperatures β-scission successfully removes many of the 2-block pillars which have formed as a result of one block adsorbing on top of another isolated block, and as the temperature increases the number of β-scission reactions also increases accordingly. But at higher temperatures the migration rate begins to exceed that of β-scission, and upper blocks are now able to migrate down (lemmings) to the lower level before β-scission can occur; thus reducing the number of β-scissions.

A check on the self-consistency of the KMC program was made by comparing the fraction of surface radical sites, F, calculated by the program with those predicted by the standard model [Eq. (3)] and our more accurate version [Eq. (2)]. Values for F were generated when the program terminated by dividing the number of activated surface blocks (red +magenta) by the total number of surface blocks (grey +green+red+magenta). The results are shown in Fig. 10. It can be seen that the standard model overestimates F quite considerably at high T_s. The more accurate KMC model reproducing Eq. (2) predicts values for F that are saturated at $T_s>1200$ K due to the reverse of reaction (R1).

VI. CONCLUSIONS

In this paper we have re-evaluated many of the fundamental steps involved in diamond CVD. We have obtained new rates for these processes and then used these for simulating diamond growth in a 1D KMC program. Direct etching of surface sp^3-bonded CH_2 or CH_3 groups is now believed to be a negligible process, because the excess energy deposited into the surface groups as a result of H addition can dissipate into the bulk before it can be used to break the C–C bond that would release the species into the gas phase. This leaves β-scission as the only viable mechanism for removal of sp^3 carbon from a growing diamond surface. However, even this process only removes $<2\%$ of the adsorbing species, meaning that the diamond growth rate is governed almost entirely by the arrival and sticking rate of carbons onto the surface. A major factor in growth is the fraction of surface radical sites available for adsorption, and this value is governed by the $[H]/[H_2]$ ratio at the surface, as well as the surface tempera-

ture (or more accurately, the gas temperature near the surface). The other important factor—the adsorption rate for CH_3 species onto the surface—has been reduced to only 15% of that used previously due to a combination of steric effects and electronic selection rules. This usefully decreases the predicted growth rate to values more in line with those seen in experiment. Migration is now seen as a much more complex process than previously believed, with the surface-diffusion length being severely limited by the lack of availability of surface radical sites. Migrating CH_2 species can hop back and forth between two adjacent radical sites thousands of times before the migration process is terminated by processes such as the radical sites or CH_2 becoming deactivated, the CH_2 attaching to a sidewall, or being etched away, etc. Thus, the overall average surface-diffusion length is <2 sites, and this has implications for both the growth rate and the surface roughness. The lemmings scenario is now the preferred pathway when a migrating group reaches the top of a step-edge. This greatly helps in reducing the build-up of columns or pillars, thereby providing an important mechanism for smoothing the surface at higher substrate temperatures. However, exclusive use of the lemmings scenario cannot reproduce some experimentally observed surface features, such as wedding cake structures, which were previously simulated using the cowards scenario. Thus, it is likely that the true scenario is a combination of lemmings and cowards, with the relative probability of each process governing the steepness of the sides of the wedding cake structures. This will be left as an item for future investigation.

The present model does not include secondary nucleation events or defects but it is still possible to make some general predictions about the conditions needed to produce SCD at high rates. For high growth rate we require high CH_3 flux to the surface, which means a high CH_4 flow rate in the gas mixture. However, for the CH_3 to adsorb we require F to be as large as possible, and this is possible by having the ratio of $[H]/[H_2]$ at the diamond surface as high as possible. This can be achieved in practice by using a dense, highly dissociated gas mixture, such as those present in a high pressure (100 Torr or more), high power (5 kW or more) microwave plasma ball localized over the substrate. A large F is also essential for rapid surface migration, the rate of which increases rapidly with substrate temperature. Rapid migration produces smoother films, so we require T_s to be as high as possible for the smoothest films. However, there is a compromise required because when T_s becomes too high, $[CH_3]$ at the surface drops, reducing the growth rate. Thus, a value of ~ 1100 K is optimal both to maximize $[CH_3]$ and to achieve smooth films. These predictions accord nicely with the conditions reported for growth of SCD by a number of groups.[53,54]

The rough texture predicted at low T_s [e.g., Fig. 6(a)] allows speculation about a possible mechanism for spontaneous segregation of the film into separated regions or islands, which may eventually grow into different grains. Thus, this may be the first suggestion of a mechanism for forming grains that simply arise from the random processes of CH_3 incorporation, CH_2 migration, surface site activation, etc., without the requirement for any renucleation event or defect formation mechanism.

In future work we shall explore these implications further and investigate the effect of defect formation and renucleation, as well as different growth conditions—such as those used to grow SCD or UNCD—upon the predicted growth rates and surface morphology. Converting the program to a full 2D geometry will also help to shed light upon aspects of the growth that depend more critically upon the exact local surface morphology, such as the shape and size of the critical nucleus, kinks and protrusions in step-edges, attachment of migrating block to inside and outside corners, migration down risers, and possible void formation.

ACKNOWLEDGMENTS

The authors wish to thank Mike Ashfold, Neil Fox, Keith Rosser, Jim Butler, and Michael Frenklach for useful discussions and suggestions. The Bristol-Moscow collaboration is supported by a Royal Society Joint Project Grant, and Y.A.M. acknowledges support from RF Government for Key Science Schools under Grant No. 3322.2010.2.

[1] P. W. May, Science **319**, 1490 (2008).
[2] P. W. May, Philos. Trans. R. Soc. London, Ser. A **358**, 473 (2000).
[3] D. G. Goodwin and J. E. Butler, in *Handbook of Industrial Diamonds and Diamond Films*, edited by M. A. Prelas, G. Popovici, L. K. Bigelow (Marcel Dekker, New York, 1998).
[4] S. J. Harris, Appl. Phys. Lett. **56**, 2298 (1990).
[5] J. E. Butler, R. L. Woodin, L. M. Brown, and P. Fallon, Philos. Trans. R. Soc. London **342**, 209 (1993).
[6] M. Frenklach and H. Wang, Phys. Rev. B **43**, 1520 (1991).
[7] P. W. May, J. N. Harvey, J. A. Smith, and Y. A. Mankelevich, J. Appl. Phys. **99**, 104907 (2006).
[8] S. Skokov, B. Weiner, M. Frenklach, T. Frauenheim, and M. Sternberg, Phys. Rev. B **52**, 5426 (1995).
[9] M. Frenklach and S. Skokov, J. Phys. Chem. B **101**, 3025 (1997).
[10] M. Frenklach, S. Skokov, and B. Wiener, Nature (London) **372**, 535 (1994).
[11] W. J. P. van Enckevort, G. Janssen, W. Vollenberg, J. J. Schermer, L. J. Giling, and M. Seal, Diamond Relat. Mater. **2**, 997 (1993).
[12] A. Cheesman, J. N. Harvey, and M. N. R. Ashfold, J. Phys. Chem. A **112**, 11436 (2008).
[13] K. Larsson and J.-O. Carlsson, Phys. Status Solidi A **186**, 319 (2001).
[14] P. W. May and Yu. A. Mankelevich, J. Phys. Chem. C **112**, 12432 (2008).
[15] S. J. Harris and D. G. Goodwin, J. Phys. Chem. **97**, 23 (1993).
[16] M. E. Coltrin and D. S. Dandy, J. Appl. Phys. **74**, 5803 (1993).
[17] B. W. Yu and S. L. Girschick, J. Appl. Phys. **75**, 3914 (1994).
[18] M. Frenklach, J. Chem. Phys. **97**, 5794 (1992).
[19] M. M. Clark, L. M. Raff, and H. L. Scott, Phys. Rev. B **54**, 5914 (1996).
[20] E. J. Dawnkaski, D. Srivastava, and B. J. Garrison, J. Chem. Phys. **104**, 5997 (1996).
[21] C. C. Battaile, D. J. Srolovitz, and J. E. Butler, J. Appl. Phys. **82**, 6293 (1997).
[22] C. C. Battaile, D. J. Srolovitz, I. I. Oleinik, D. G. Pettifor, A. P. Sutton, S. J. Harris, and J. E. Butler, J. Chem. Phys. **111**, 4291 (1999).
[23] J. C. Angus, M. K. Sunkara, S. R. Sahaida, and J. T. Glass, J. Mater. Res. **7**, 3001 (1992).
[24] R. C. Mani and M. K. Sunkara, Diamond Relat. Mater. **12**, 324 (2003).
[25] C. C. Battaile and D. J. Srolovitz, Annu. Rev. Mater. Res. **32**, 297 (2002).
[26] A. Netto and M. Frenklach, Diamond Relat. Mater. **14**, 1630 (2005).
[27] P. W. May, N. L. Allan, J. C. Richley, M. N. R. Ashfold, and Yu. A. Mankelevich, J. Phys.: Condens. Matter **21**, 364203 (2009).
[28] A. Pimpinelli and J. Villain, *Physics of Crystal Growth* (Cambridge University Press, Cambridge, UK, 1998).
[29] G. Ehrlich and F. G. Hudda, J. Chem. Phys. **44**, 1039 (1966).
[30] R. L. Schwoebel, J. Appl. Phys. **40**, 614 (1969).

[31]P. W. May, N. L. Allan, M. N. R. Ashfold, J. C. Richley, and Yu. A. Mankelevich, Diamond Relat. Mater. **19**, 389 (2010).
[32]M. Eckert, E. Neyts, and A. Bogaerts, Cryst. Eng. Comm. **11**, 1597 (2009).
[33]M. Eckert, E. Neyts, and A. Bogaerts, Cryst Growth Des. (to be published).
[34]Yu. A. Mankelevich, M. N. R. Ashfold, and J. Ma, J. Appl. Phys. **104**, 113304 (2008).
[35]T. V. Regemorter and K. Larsson, J. Phys. Chem. A **112**, 5429 (2008).
[36]S. J. Klippenstein, Y. Georgievskii, and L. B. Harding, Phys. Chem. Chem. Phys. **8**, 1133 (2006).
[37]N. Setaka, J. Mater. Res. **4**, 664 (1989).
[38]R. E. Rawles, S. F. Komarov, R. Gat, W. G. Morris, J. B. Hudson, and M. P. D'Evelyn, Diamond Relat. Mater. **6**, 791 (1997).
[39]R. E. Stallcup II and J. M. Perez, Phys. Rev. Lett. **86**, 3368 (2001).
[40]C. M. Donnelly, R. W. McCullough, and J. Geddes, Diamond Relat. Mater. **6**, 787 (1997).
[41]A. Cheesman, J. N. Harvey, and M. N. R. Ashfold, Phys. Chem. Chem. Phys. **7**, 1121 (2005).
[42]H. Eyring, J. Chem. Phys. **3**, 107 (1935).
[43]J. C. Richley, J. N. Harvey, and M. N. R. Ashfold, in *Diamond Electronics and Bioelectronics: Fundamentals to Applications III*, MRS Symposia Proceedings No. 1203 edited by P. Bergonzo, J. E. Butler, R. B. Jackman, K. P. Loh, and M. Nesládek (Materials Research Society, Warrendale, PA, 2010), p. J17-32.
[44]P. Martineau, M. Gaukroger, R. Khan, and D. Evans, Phys. Status Solidi C **6**, 1953 (2009).
[45]K. Larsson and J.-O. Carlsson, Phys. Rev. B **59**, 8315 (1999).
[46]Yu. A. Mankelevich and P. W. May, Diamond Relat. Mater. **17**, 1021 (2008).
[47]J. E. Butler, Yu. A. Mankelevich, A. Cheesman, J. Ma, and M. N. R. Ashfold, J. Phys.: Condens. Matter **21**, 364201 (2009).
[48]J. C. Richley, J. N. Harvey, and M. N. R. Ashfold, J. Phys. Chem. A **113**, 11416 (2009).
[49]S. Skokov, B. Weiner, and M. Frenklach, J. Phys. Chem. **98**, 7073 (1994).
[50]D. R. Alfonso, S. H. Yang, and D. A. Drabold, Phys. Rev. B **50**, 15369 (1994).
[51]A. B. Bortz, M. H. Kalos, and J. L. Lebowitz, J. Comput. Phys. **17**, 10 (1975).
[52]E. Kondoh, T. Ohta, T. Mitomo, and K. Ohtsuka, Appl. Phys. Lett. **59**, 488 (1991).
[53]G. Bogdan, K. De Corte, W. Deferme, K. Haenen, and M. Nesládek, Phys. Status Solidi A **203**, 3063 (2006).
[54]C.-s. Yan, H.-k. Mao, W. Li, J. Qian, Y. Zhao, and R. J. Hemley, Phys. Status Solidi A **201**, R25 (2004).
[55]P. W. May, M. N. R. Ashfold, and Yu. A. Mankelevich, J. Appl. Phys. **101**, 053115 (2007).